

# Effects of the spin-orbital coupling on the vacancy-induced magnetism on the honeycomb lattice

Weng-Hang Leong, Shun-Li Yu, and Jian-Xin Li

*National Laboratory of Solid State Microstructure and Department of Physics, Nanjing University, Nanjing 210093, China*

(Dated: October 7, 2018)

The local magnetism induced by vacancies in the presence of the spin-orbital interaction is investigated based on the half-filled Kane-Mele-Hubbard model on the honeycomb lattice. Using the self-consistent mean-field theory, we find that the spin-orbital coupling will enhance the localization of the spin moments near a single vacancy. We further study the magnetic structures along the zigzag edges formed by a chain of vacancies. We find that the spin-orbital coupling tends to suppress the counter-polarized ferrimagnetic order on the upper and lower edges, because of the open of the spin-orbital gap. As a result, in the case of the balance number of sublattices, it will suppress completely this kind of ferrimagnetic order. But, for the imbalance case, a ferrimagnetic order along both edges exists because additional zero modes will not be affected by the spin-orbital coupling.

## I. INTRODUCTION

Graphene and related nanostructured materials have attracted much interest in solid state physics recently due to their bidimensional character and a host of peculiar properties<sup>1</sup>. Among them, the investigation of the magnetic properties in graphene is one of the fascinating topics, as no  $d$  and  $f$  elements are necessary in the induction of magnetism in comparison with the usual magnetic materials. Theoretical predictions and experimental investigations have revealed that a nonmagnetic defect such as an impurity or a vacancy can induce the non-trivial localized magnetism<sup>2-6</sup>. Similarly, a random arrangement of a large number of vacancies which are generated by the high-dose exposure of graphene to strong electron irradiation<sup>7</sup> can also induce magnetism theoretically<sup>8</sup>. These studies not only have the fundamental importance, but also open a door for the possibility of application in new technologies for designing nanoscale magnetic and spin electronic devices.

On the other hand, the topological insulating electronic phases driven by the spin-orbital (SO) interaction have also attracted much interest recently. The Kane-Mele model for the topological band insulator is defined on the honeycomb lattice<sup>9,10</sup> which is the same lattice structure as graphene. Possible realization of an appreciable SO coupling in the honeycomb lattice includes the cold fermionic atoms trapped in an extraordinary optical lattice<sup>11</sup>, the transition-metal oxide  $\text{Na}_2\text{IrO}_3$ <sup>12</sup> and the ternary compounds such as  $\text{LiAuSe}$  and  $\text{KHgSb}$ <sup>13</sup>. Topological band insulator has a nontrivial topological order and exhibits a bulk energy gap with gapless, helical states at the edge<sup>14-16</sup>. These edge states are protected by the time reversal symmetry and are robust with respect to the time-reversal symmetric perturbations, such as nonmagnetic impurities. It is shown that a vacancy, acting as a minimal circular inner edge, will induce novel time-reversal invariant bound states in the band gap of the topological insulator<sup>17-19</sup>. Theoretically, it is also shown that the SO coupling suppresses the edge magnetism induced in the zigzag ribbon of the honeycomb lattice in

the presence of electron-electron interactions<sup>20</sup>. Thus, it is expected that the SO coupling would also affect the local magnetism in the bulk induced by vacancies.

In this paper, we study theoretically the effects of the SO coupling on the local magnetism induced by a single and a multi-site vacancy on the honeycomb lattice, based on the Kane-Mele-Hubbard model where both the SO coupling and the Hubbard interaction between electrons are taken into consideration. This model has been extensively studied to explore the effect of the strong correlation on the topological insulators<sup>21-27</sup>. Making use of the self-consistent mean field approximation, we calculate the local spin moments and their distribution around the vacancies. For a single vacancy, we find that the main effect of the SO coupling is to localize the spin moments to be near the vacancy, so that it will enhance the local spin moments. For a large stripe vacancy by taking out a chain of sites from the lattice, we find that the SO coupling tends to suppress the counter-polarized ferrimagnetic order induced along the zigzag edges, because of the open of the SO gap. As a result, in the case of the balance number of sublattices (with even number of vacancies), the SO coupling will suppress completely the counter-polarized ferrimagnetic order along the upper and lower edges. While, in the case of the imbalance number of sublattices (with odd number of vacancies), a ferrimagnetic order along both edges exists because additional zero modes will not be affected by the SO coupling.

We will introduce the model and the method of the self-consistent mean-field approximation in Sec.II. In Sec.III and IV, we present the results for a single vacancy and a multi-site vacancy, respectively. Finally, a brief summary will be given in Sec.V.

## II. MODELS AND COMPUTATIONAL METHODS

We start from the Kane-Mele model<sup>9</sup>, in which the intrinsic SO coupling with a coupling constant  $\lambda$  is in-

cluded.

$$H_0 = -t \sum_{\langle ij \rangle, \sigma} c_{i\sigma}^\dagger c_{j\sigma} + i\lambda \sum_{\langle\langle ij \rangle\rangle \sigma\sigma'} v_{ij} \sigma_{\sigma\sigma'}^z c_{i\sigma}^\dagger c_{j\sigma'}, \quad (1)$$

where  $c_{i\sigma}^\dagger$  ( $c_{j\sigma}$ ) is the creation(annihilation) operator of the electron with spin  $\sigma$  on the lattice site  $i$ ,  $\langle ij \rangle$  represents the pairs of the nearest neighbor sites (the hopping is  $t$ ) and  $\langle\langle ij \rangle\rangle$  those of the next-nearest neighbors.  $v_{ij} = +1(-1)$  if the electron makes a left(right) turn to get to the second bond. The size of our system is considered to be finite with periodic boundary condition. So, the position of each lattice site can be described specifically by  $i = \Gamma(m, n)$ , representing that the lattice site  $i$  is in the  $m$ th column and the  $n$ th row, and  $\Gamma = A, B$  the sublattice labels. The number of the unit cells is denoted by  $N_c = L^2$ , therefore the total number of the lattice sites is  $N_l = 2L^2$ . To consider the correlation between electrons, we will include the Hubbard term in the Hamiltonian, which is given by  $H_I$ ,

$$H_I = U \sum_i \hat{n}_{i\uparrow} \hat{n}_{i\downarrow}, \quad (2)$$

where  $\hat{n}_{i\sigma} = c_{i\sigma}^\dagger c_{i\sigma}$ . When vacancies are introduced, the hoppings between the vacancy and the nearest neighbors and the on-site interaction on that vacancy are subtracted from the overall Hamiltonian. Hence the corresponding number of the lattice sites is  $N_l = 2L^2 - N_v$ , where  $N_v$  is the number of vacancies. The total number of electrons  $N_e$  is fixed to be at the half-filling ( $N_e = N_l$ ). The Hubbard interaction term is treated with the self-consistent mean field approximation, so that we will obtain an effective single-particle Hamiltonian where the electrons interact with a spin-dependent potential,

$$H_I \simeq U \sum_{i,\sigma} \langle \hat{n}_{i-\sigma} \rangle \hat{n}_{i\sigma} - U \sum_i \langle \hat{n}_{i\uparrow} \rangle \langle \hat{n}_{i\downarrow} \rangle. \quad (3)$$

And the overall mean field Hamiltonian  $H_{mf}$  is then given by,

$$H_{mf} = U \sum_{i\sigma} \langle \hat{n}_{i-\sigma} \rangle \hat{n}_{i\sigma} + H_0. \quad (4)$$

After diagonalizing the Hamiltonian  $H_{mf}$ , we can determine the occupation number  $\langle \hat{n}_{i-\sigma} \rangle$  at each site with different spins using the eigenvectors of  $H_{mf}$ , and this process is carried out iteratively until a required accuracy is reached. Then the magnetic moment of each site  $m_i = \langle \hat{n}_{i\uparrow} - \hat{n}_{i\downarrow} \rangle$  can be calculated. We note that a collinear magnetic texture is assumed in our system, as used before for the investigations of Kane-Mele-Hubbard model<sup>20,21</sup>. We have checked the results with the non-collinear magnetic texture and found that the collinear magnetic texture is favored.

### III. MAGNETISM WITH ONE VACANCY

The calculation is carried out on the lattice with  $N_c = 14 \times 14$  unit cells in which a single vacancy is introduced

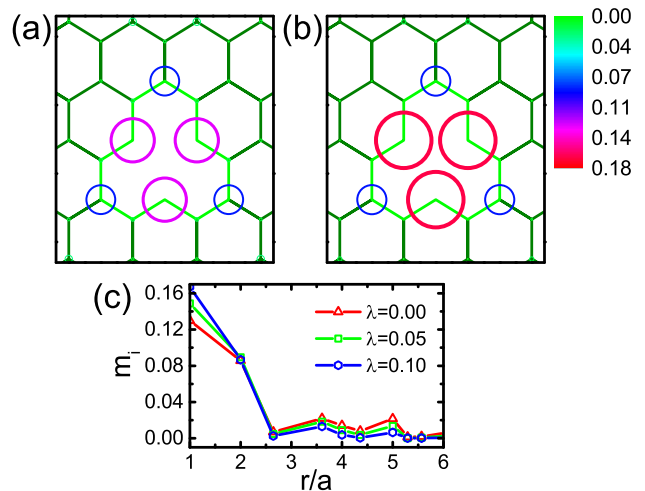


FIG. 1: (color online). (a) and (b): Distribution of the spin moments  $m_i$  on lattice sites around a single vacancy at  $A(7, 7)$  with  $U = 1.0t$ , in which (a) corresponds to the SO coupling constant  $\lambda = 0.0$  and (b)  $\lambda = 0.1t$ . The area and color of the hollow circles represent the magnitude of the spin moments. (c)  $m_i$  on the  $B$  sublattice as a function of the distance  $r$  away from the vacancy. The unit  $a$  is the distance between the nearest sites.

on the site  $A(7, 7)$ . Figure 1 displays the distribution of the magnetic moment when the Hubbard interaction is taken to be  $U = 1.0t$ , in which the size and the color of the circle on each lattice site denote the magnitude of the local spin moment. From Fig.1(a) where the SO coupling is turned off, one can see that localized magnetic moments are induced around the vacancy in the presence of a finite Hubbard interaction  $U$ . This is in agreement with the prediction of the Lieb theorem<sup>28</sup> regarding the total spin  $S$  of the exact ground state of the Hubbard model on bipartite lattices. It states that the total spin  $S$  is given by the sublattice imbalance  $2S = |N_A - N_B|$ , with  $N_A$  and  $N_B$  the number of atoms belonging to each sublattice. With the introducing of a single vacancy on the  $A$  sublattice, an imbalance  $N_B - N_A = 1$  appears and a magnetic structure near the vacancy with the total spin  $S = 1/2$  will form. Similar results have also been obtained in recent studies in graphene<sup>2-4</sup>.

In the presence of the SO coupling, the magnitude of the magnetic moments around the vacancy increases, as shown in Fig. 1(b) for  $\lambda = 0.1t$ . At the meantime, if we check the distribution of the magnetic moments, as shown in Fig.1(c) where the magnitude of the magnetic moments on sublattice  $B$  as a function of the distance  $r$  away from the vacancy is presented, one will find that the magnetic moments are more localized with the increase of the SO coupling. These features demonstrate that the SO coupling will enhance the magnetic moments near the vacancy notably.

In order to show the emergence of the magnetism induced by the vacancy in more detail, we calculate the

spin resolved local density of state(LDOS) as defined by,

$$D_{\sigma}(\epsilon) = \sum_{n,i} |u_{i,\sigma}^n|^2 \delta(\epsilon - \epsilon_n), \quad (5)$$

where  $i$  runs over the lattice sites surrounding the vacancy up to the third-nearest neighbors, as those linked by the green line in Fig.1(a) and (b).  $u_{i,\sigma}^n$  is the single-particle amplitude on the  $i$ th site with spin  $\sigma$  and the corresponding eigenvalue is  $\epsilon_n$ . The Delta function in Eq.(2) is replaced by the Lorentzian function for plotting. The results for the LDOS are presented in Fig. 2(a)-(h) for different Hubbard interaction  $U$  and SO interaction  $\lambda$ . The red and blue lines represent the LDOS for the spin up and spin down components respectively, and the dash lines show the LDOS away from the vacancy for a comparison. In the case of  $U = \lambda = 0.0$  as shown in Fig. 2(a), the LDOS shows a V-shape linear behavior near the Fermi level for those lattice sites far away from the vacancy (denoted by the dashed line) which is the consequence of the linear dispersion relation of the electrons, the so-called Dirac fermions. For those around the vacancy, a peak at the Fermi level emerges as shown by

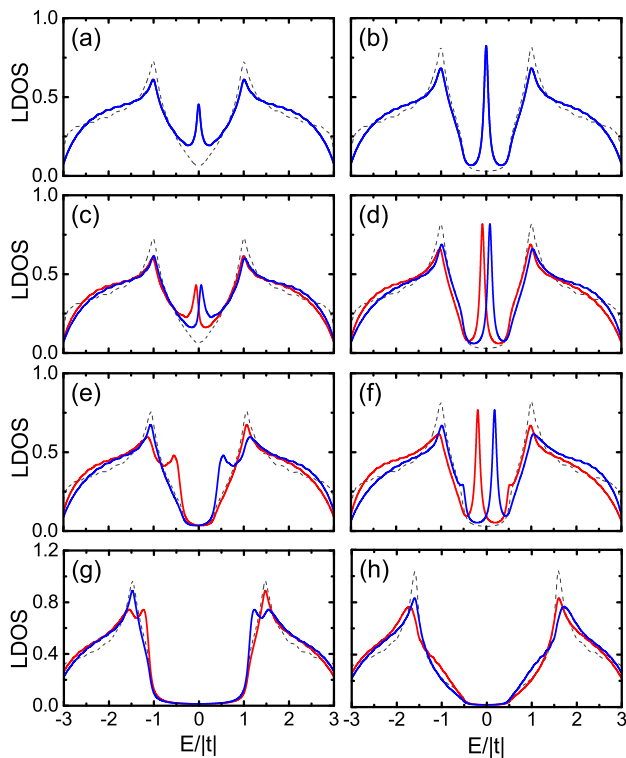


FIG. 2: (color online). LDOS for  $\lambda = 0.0$  [left column, including (a),(c),(e),(g)] and for  $\lambda = 0.1t$  [right column, including (b),(d),(f),(h)], where the Hubbard interaction  $U = 0.0$  for (a) and (b),  $U = 1.6t$  for (c) and (d),  $U = 2.6t$  for (e) and (f), and  $U = 3.6t$  for (g) and (h), respectively. LDOS for different spins is resolved, those with the spin up are denoted by the blue lines and the spin down the red lines. The grey dash lines represent the LDOS on the lattice site away from the vacancy.

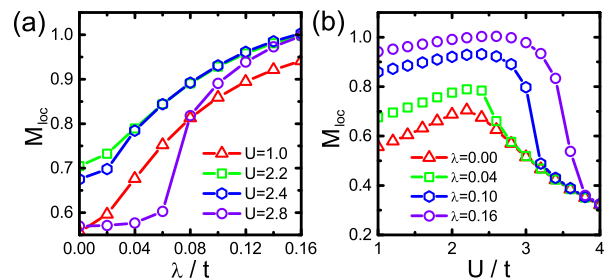


FIG. 3: (color online). Local moments  $M_{loc}$  (see text) are shown as a function of the SO coupling  $\lambda$  for different Hubbard interaction  $U$  (a) and of  $U$  for different  $\lambda$  (b).

the solid line, which corresponds to the localized states induced by the vacancy<sup>29</sup>. After turning on the SO coupling, such as that for  $\lambda = 0.1t$  [see Fig.2(b)], we can see that an energy gap opens for those lattice sites far away from the vacancy<sup>9,10</sup>, so that now a U-shape LDOS near the Fermi level occurs. In this way, the mid-gap peak is enhanced noticeably because the decay rate of the localized states into the continuum is reduced largely due to the open of the energy gap. This will lead to the increase in the spectral weight of the localized states around the vacancy. However, for both cases, one will find that the LDOS for the spin up and spin down components degenerates, so that the system will not show magnetism as a whole without the Hubbard interaction.

The effect of a finite Hubbard interaction  $U$  is to split the spin degenerate LDOS, so that two peaks occur corresponding to different spins, as shown in Fig. 2(c)-(f). Consequently, the localized spin up and down moments will not cancel out in this case, and a net magnetism around the vacancy is induced.

The magnetism may be quantified by the local moment  $M_{loc} = \sum_i m_i$ , where the sum runs over the lattice sites surrounding the vacancy up to the third-nearest neighbors as used above in the calculation for the LDOS. The results are presented in Fig. 3(a) and (b) for different  $U$  and  $\lambda$ , respectively. The local moment  $M_{loc}$  shows a monotonic increase with the SO coupling  $\lambda$ , so it reinforces our observation that the local magnetism is enhanced by the SO coupling as shown in Fig.1. On the other hand,  $M_{loc}$  shows a nonmonotonic dependence on the Hubbard interaction  $U$ , namely it increases with  $U$  firstly and then decreases with a further increase of  $U$  after a critical value  $U_c$ . As discussed above, the local magnetism is determined by the spin-split localized states induced by the vacancy, and it is the Hubbard interaction  $U$  to split the spin-degenerate states. Because the open of the gap due to the SO coupling will decrease the decay rate of the localized states into the continuum, so it will enhance the spectral weight of the localized states [see also Fig. 2], consequently the localized magnetism. The splitting between the two localized states with different spins is proportional to  $U$ , so the two split

localized states will situate in the SO gap for a small  $U$ [Fig. 2(c)-(f)]. However, when  $U > U_c$  the splitting will be larger than the SO gap, and it pushes the localized states to merge into the continuum[Fig.2(g) and (h)], so the local magnetism will decrease.

#### IV. THE CASE OF MULTI-SITE VACANCY

The multi-site vacancy can be formed by removing the sites continuously. Here, we consider a large stripe vacancy by taking out a chain of sites from the lattice as illuminated in Fig. 4. In this way, the stripe vacancy consists of one upper and one lower zigzag edges. As clarified by the Lieb theorem<sup>28</sup>, the sublattice imbalance between the number of atoms belonging to different sublattices will have significant effect on the magnetism. For the stripe vacancy considered here, the imbalance is expressed by the parity of the number of vacancies, where the number is even ( $N_A = N_B$ ) in Fig. 4(a) and (b), and odd ( $N_A \neq N_B$ ) in Fig. 4(c) and (d), thus the total spin of the system is  $S = 0$  and  $1/2$  respectively.

In the case of even number of vacancies, a ferrimagnetic spin order emerges on both the upper and lower zigzag edges around the stripe vacancies when there is no SO coupling, as shown in Fig. 4(a). The ferrimagnetic arrangement and the magnitude of the spin moments on these two edges are symmetric, but they are counter-polarized, so they cancel out exactly and the whole system will not show magnetism. This is consistent with the Lieb theorem<sup>28</sup>. The ferrimagnetic order on a sufficiently long zigzag edge around the stripe vacancies here is similar to the spin order formed at the outer edge of the zigzag ribbon<sup>30-33</sup> and the graphene nanoisland<sup>34</sup>. In the case of odd number of vacancies, a similar ferrimagnetic spin order is also induced with a slightly large magnitude [Fig. 4(c)]. Interestingly, this ferrimagnetic order occurs only on the upper zigzag edge, not on the lower edge. This phenomenon is ascribed to the presence of an extra spin when a sublattice imbalance  $N_A \neq N_B$  exists, as

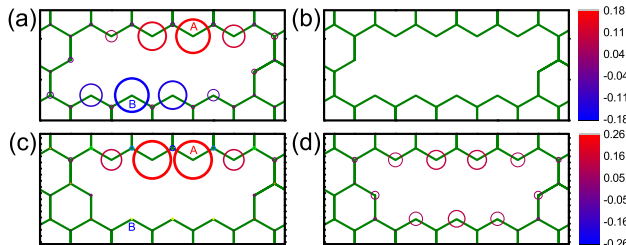


FIG. 4: (color online). Distribution of the spin moments  $m_i$  on the lattice sites surrounding the vacancies for  $U = 1.0t$  and  $L = 14$ . A cluster of vacancies is formed with the number of missing sites for (a), (b)  $N_v = 8$  and (c), (d)  $N_v = 7$ . SO coupling is set to be  $\lambda = 0.0$  for (a), (c) and  $\lambda = 0.1t$  for (b), (d). The area and color of hollow circles represent the magnitude of the moments.

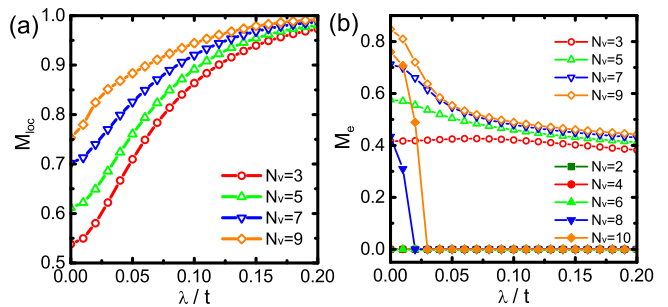


FIG. 5: (color online). (a) Local moments  $M_{loc}$  are plotted as a function of  $\lambda$  while  $U = 1.0t$  and  $L = 14$ . The function in different size of vacancy is distinguished by different color and shape of points. The cases of even  $N_v$  are not plotted as local moments are always zero obeying Lieb theorem<sup>28</sup>. (b) The function of edge moments  $M_e$  versus  $\lambda$  are given in different  $N_v$ .

described by the Lieb theorem<sup>28</sup>.

After turning on the SO coupling, such as for  $\lambda = 0.1t$ , the ferrimagnetic spin order on both the upper and lower zigzag edges around the stripe vacancies disappears completely in the case of even number of vacancies[Fig. 4(b)]. However, the effect of the SO coupling on local magnetism is quite different for the case of an odd number of vacancies. Here, a ferrimagnetic spin order similar to that on the upper edge emerges on the lower edge, though the magnitude of the individual spin moment is reduced[Fig. 4(d)]. To show variation of the total magnetism, we plot the quantity  $M_{loc}$  as a function of the SO coupling  $\lambda$  in Fig. 5(a), here  $M_{loc}$  is the sum of the spin moments on the sites which are on the zigzag edges around the vacancies. Since  $M_{loc}$  is always zero in the case of even  $N_v$ , it is not plotted here. With an odd  $N_v$ , the local moment  $M_{loc}$  increases with the increase of  $\lambda$ , which shows a similar behavior as that in the case of a single vacancy. This indicates that the total local magnetism shown in Fig. 4(d) is in fact enhanced with the introduction of the SO coupling and approaches the saturation value 1 finally. From Fig. 5(a), one can also find that  $M_{loc}$  increases with the increase of the number of vacancies  $N_v$ . This suggests that the SO coupling will localize the induced spin moments to those lattice sites which are neighboring the vacancies.

To quantify the variation of the spin moments with  $\lambda$  on the upper zigzag edge, we also present  $M_e$  as a function of  $\lambda$  in Fig. 5(b), here  $M_e$  is the sum of the spin moments only on the sites on the upper zigzag edge. Let us consider firstly the case of even number of  $N_v$ , for a small number of even vacancies,  $M_e$  is always zero. Up to  $N_v \geq 8$ , a finite  $M_e$  occurs and it increases with  $N_v$  by the formation of the zigzag edges. However,  $M_e$  drops rapidly to zero after turning on the SO coupling. These results quantify the physical picture derived from Fig. 4(a) and (b). Now let us turn to the case of odd number of  $N_v$ . Without the SO coupling,  $M_e$  also shows

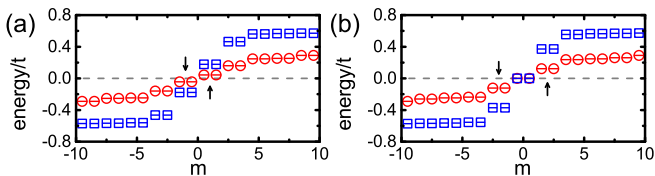


FIG. 6: (color online). The single-particle energy levels labeled with  $m$  (see text) near the Fermi level of the non-interacting systems for (a)  $N_v = 8$  and (b)  $N_v = 7$ . SO coupling is set to be  $\lambda = 0.0$  for the red circles and  $\lambda = 0.1t$  for the blue squares.

an increase with  $N_v$ . With the introduction of the SO coupling,  $M_e$  shows a decrease with  $\lambda$  and saturates to near one half of  $M_{loc}$ .

In fact, we can make an analogy between the stripe vacancy and the graphene ribbon with zigzag edges. A remarkable feature of the graphene ribbon with zigzag edges is that it has a flat band localized on the zigzag edge<sup>1</sup>. An important effect of this flat band is that a counter-polarized ferromagnetic order along the upper and lower edges will be induced when the Hubbard interaction between electrons is included<sup>30-33</sup>. In view of this, we plot the single-particle spectra for the systems with the stripe vacancy without the Hubbard interaction in Fig.6(a) and (b) for  $N_v = 8$  and  $N_v = 7$ , respectively. Each energy level is labeled with  $m = n - N_e - 1/2$  in order to indicate that the energy level with  $m < 0$  is occupied by electron. For the systems without SO coupling, we find that there are four near-degeneracy localized states [red circles indicated by arrows in Fig.6(a) and (b)] which is near the Fermi level for both  $N_v = 8$  and  $N_v = 7$ . These states will have the same effect as the flat band in the zigzag ribbon when a suitable Hubbard  $U$  is turned on. So, a counter-polarized ferrimagnetic order as shown in Fig.4(a) will emerge. However, we note that there are two additional zero modes for  $N_v = 7$  relative to  $N_v = 8$ , due to the imbalance between the sublattices

( $N_A > N_B$ ). These zero modes will induce extra spin moments on both edges, which counteract the antiparallel moments on the lower edge. Thus, in the case of  $N_v = 7$ , only the ferrimagnetic order on the upper edge appears. After turning on the SO coupling, those localized states [blue squares indicated by arrows in Fig.6(a) and (b)] are pushed away from the Fermi level due to the open of the SO gap. Thus, as shown in Fig.4(b), a small Hubbard  $U$  is not enough to induce the counter-polarized ferrimagnetic order on the upper and lower edges. However, the zero modes originating from the imbalance of sublattices are not affected by the SO coupling [Fig.6(b)]. So, the additional ferrimagnetic order on both edges induced by these zero modes will remain for  $N_v = 7$ .

## V. CONCLUSION

In a summary, we have studied the local magnetism induced by vacancies on the honeycomb lattice based on the Kane-Mele-Hubbard model. It is shown that the SO coupling tends to localize and consequently enhances the local magnetic moments near a single vacancy. Furthermore, along the zigzag edges formed by a chain of vacancies, the SO coupling will suppress completely the counter-polarized ferrimagnetic order along the edges. Therefore, the system will not show any local magnetism in the case of even number of vacancies. For an odd number of vacancies, a ferrimagnetic order along both edges exists and the total magnetic moments along both edges will increase.

## Acknowledgments

This work was supported by the National Natural Science Foundation of China (Grant Nos. 91021001, 11190023 and 11204125) and the Ministry of Science and Technology of China (973 Project grant numbers 2011CB922101 and 2011CB605902).

<sup>1</sup> A. H. C. Neto, F. Guinea, N. M. R. Peres, K. S. Novoselov, and A. K. Geim, *Rev. Mod. Phys.* **81**, 109 (2009).  
<sup>2</sup> O. V. Yazyev and L. Helm, *Phys. Rev. B* **75**, 125408 (2007).  
<sup>3</sup> H. Kumazaki and D. S. Hirashima, *J. Phys. Soc. Jpn.* **76**, 064713 (2007).  
<sup>4</sup> O. V. Yazyev, *Phys. Rev. Lett.* **101**, 037203 (2008).  
<sup>5</sup> M. M. Ugeda, I. Brihuega, F. Guinea, and J. M. Gómez-Rodríguez, *Phys. Rev. Lett.* **104**, 096804 (2010).  
<sup>6</sup> R. R. Nair, M. Sepioni, I.-L. Tsai, O. Lehtinen, J. Keinonen, A. V. Krasheninnikov, T. Thomson, A. K. Geim, and I. V. Grigorieva, *Nature Phys.* **8**, 199-202 (2012).  
<sup>7</sup> J. Kotakoski, A. V. Krasheninnikov, U. Kaiser, and J. C. Meyer, *Phys. Rev. Lett.* **106**, 105505 (2011).  
<sup>8</sup> J. J. Palacios, J. Fernández-Rossier, and L. Brey, *Phys. Rev. B* **77**, 195428 (2008).

<sup>9</sup> C. L. Kane and E. J. Mele, *Phys. Rev. Lett.* **95**, 146802 (2005).  
<sup>10</sup> C. L. Kane and E. J. Mele, *Phys. Rev. Lett.* **95**, 226801 (2005).  
<sup>11</sup> K. L. Lee, B. Gremaud, R. Han, B. G. Englert, and C. Miniatura, *Phys. Rev. A* **80**, 043411 (2009).  
<sup>12</sup> A. Shitade, H. Katsura, J. Kunes, X. -L. Qi, S. -C. Zhang, and N. Nagaosa, *Phys. Rev. Lett.* **102**, 256403 (2009).  
<sup>13</sup> H. -J. Zhang, S. Chadov, L. Müchler, B. Yan, X. -L. Qi, J. Kübler, S. -C. Zhang, and C. Felser, *Phys. Rev. Lett.* **106**, 156402 (2011).  
<sup>14</sup> B. A. Bernevig, T. A. Hughes, and S. C. Zhang, *Science* **314**, 1757 (2006).  
<sup>15</sup> M. König, Wiedemann, C. Brüne, A. Roth, H. Buhmann, L. W. Molenkamp, X. L. Qi, and S. C. Zhang, *Science* **318**, 766 (2007).

- <sup>16</sup> M. Z. Hasan and C. L. Kane, *Rev. Mod. Phys.* **82**, 3045 (2010).
- <sup>17</sup> W. -Y. Shan, J. Lu, H. -Z. Lu, and S. -Q. Shen, *Phys. Rev. B* **84**, 035307 (2011).
- <sup>18</sup> J. W. González and J. Fernández-Rossier, *Phys. Rev. B* **86**, 115327 (2012).
- <sup>19</sup> J. He, Y. -X. Zhu, Y. -J. Wu, L. -F. Liu, Y. Liang, and S. -P. Kou, *Phys. Rev. B* **87**, 075126 (2013).
- <sup>20</sup> D. Soriano and J. Fernández-Rossier, *Phys. Rev. B* **82**, 161302(R) (2010).
- <sup>21</sup> S. Rachel and K. Le Hur, *Phys. Rev. B* **82**, 075106 (2010).
- <sup>22</sup> M. Hohenadler, T. C. Lang, and F. F. Assaad, *Phys. Rev. Lett.* **106**, 100403 (2011).
- <sup>23</sup> S. L. Yu, X. C. Xie, and J. X. Li, *Phys. Rev. Lett.* **107**, 010401 (2011).
- <sup>24</sup> D. Zheng, G. M. Zhang, and C. Wu, *Phys. Rev. B* **84**, 205121 (2011).
- <sup>25</sup> W. Wu, S. Rachel, W. M. Liu, and K. Le Hur, *Phys. Rev. B* **85**, 205102 (2012).
- <sup>26</sup> C. Griset and C. Xu, *Phys. Rev. B* **85**, 045123 (2012).
- <sup>27</sup> J. Wen, M. Kargarian, A. Vaezi, and G. A. Fiete, *Phys. Rev. B* **84**, 235149 (2011).
- <sup>28</sup> E. H. Lieb, *Phys. Rev. Lett.* **62**, 1201 (1989).
- <sup>29</sup> V. M. Pereira, F. Guinea, J. M. B. Lopes dos Santos, N. M. R. Peres, and A. H. Castro Neto, *Phys. Rev. Lett.* **96**, 036801 (2006).
- <sup>30</sup> M. Fujita, K. Wakabayashi, K. Nakada, and K. Kusakabe, *J. Phys. Soc. Jpn.* **65**, 1920 (1996).
- <sup>31</sup> K. Wakabayashi, M. Sigrist, and M. Fujita, *J. Phys. Soc. Jpn.* **67**, 2089 (1998).
- <sup>32</sup> Y. W. Son, M. L. Cohen, and S. G. Louie, *Phys. Rev. Lett.* **97**, 216803 (2006).
- <sup>33</sup> J. Fernández-Rossier, *Phys. Rev. B* **77**, 075430 (2008).
- <sup>34</sup> J. Fernández-Rossier and J. J. Palacios, *Phys. Rev. Lett.* **99**, 177204 (2007).